







A COMPARATIVE STUDY OF MICROSTRUCTURE AND PROPERTIES OF MULTICOMPONENT COATINGS BASED ON (TiZrSiY)N SYSTEM PREPARED BY THE VACUUM ARC DEPOSITION[†]

 Vyacheslav M. Beresnev^a,  Serhii V. Lytovchenko^{a*},  Mykola O. Azarenkov^{a,b},
 Olga V. Maksakova^a,  Denis V. Horokh^a,  Bohdan O. Mazilin^a

^a V.N. Karazin Kharkiv National University
4, Svobody Sq., 61022 Kharkiv, Ukraine

^b National Science Center "Kharkov Institute of Physics and Technology"
1, Akademicheskaya St., 61108 Kharkiv, Ukraine

^{*}Corresponding Author e-mail: s.lytovchenko@karazin.ua

Received July 10, 2023; revised August 7, 2023; accepted August 10, 2023

The effect of reaction gas (nitrogen) pressure on the structural-phase state and properties of vacuum-arc nitride coatings of (TiZrSiY)N system has been studied. On the surface of the coatings, a significant amount of the droplet fraction and solidified macroparticles of the sputtered cathode is observed, which is typical for vacuum-arc condensates obtained from unseparated plasma flows. In all samples, titanium nitride with a cubic fcc lattice is identified. In the coating obtained at nitrogen pressures 0.08 Pa and 0.2 Pa, the α -Ti phase was determined, and the measured lattice parameter of this phase suggests that it is a solid solution of nitrogen in titanium. The texture coefficient of the multicomponent coating obtained at the highest nitrogen pressure of 0.55 Pa has the highest value of 5.95 compared to others. The Vickers hardness of multicomponent coatings increases depending on the partial pressure of nitrogen from 25.0 GPa to 36.0 GPa. According to the complex of tribo-mechanical parameters (hardness, elastic modulus, elastic strain to failure, friction coefficient etc.), suggested multicomponent (TiZrSiY)N coatings can be very attractive for tribological applications.

Keywords: Vacuum-arc coatings; Multicomponent nitride coatings; Nitrogen partial pressure; Texture; Vickers hardness; Adhesive strength

PACS: 61.46.-w; 62.20.Qp; 62-25.-g; 81.15.Cd

INTRODUCTION

The formation of functional coatings on the surface of various materials is an effective method for improving their performance under various thermobaric impacts. The high mechanical properties of the coating, combined with the thermal stability of the protective layer, can provide the necessary long-term performance of various machine parts, cutting tools, friction pairs, and other elements of different devices. However, practical experiments have shown that with an increase in specific loads, worsening in some cases of lubrication conditions for parts, tightening of requirements for the reliability and durability of various parts and products, coatings based on simple refractory compounds cease to meet the put forward requirements.

An effective approach that allows, on the one hand, to significantly change the physical and mechanical properties of the coatings, and, on the other hand, to improve the performance characteristics of structural materials on which such coatings are deposited, is the use of coatings based on multicomponent systems. Such coatings can be obtained by alloying well-known coatings based on nitrides and carbides of the refractory metals with the specific elements that provide increased surface hardness, low coefficient of friction, good adhesion to the substrate, oxidation resistance, and wear resistance [1–5]. The deposition method of such systems is based on the fact that a multicomponent system can be obtained in the state of a solid single-phase substitution solution, which by its nature is both stronger and more thermodynamically stable compared to a multi-phase solution.

The physical and mechanical characteristics of nitride coatings based on multicomponent systems mainly depend on the amount of nitride-forming elements in the system, as well as on the method and technological parameters of deposition.

A positive increase in properties can be achieved by selecting such a number of components and such a ratio of their concentrations in the material, at which an increased value of the mixing entropy is realized in the calculated composition (therefore, according to the Gibbs equation, a reduced free energy of the system). At the same time, such a value of entropy exists not only in the molten state, but also after solidification. The decrease in free energy causes an increased resistance of the solid solution during subsequent heat treatment [6]. The improved mechanical characteristics at high temperatures are realized due to a strong distortion of the crystal lattice (usually bcc) due to differences in the values of the atomic radii of the substitution elements. In this case, the higher the mixing entropy, the more pronounced the indicated characteristics of the multicomponent material. The use of multicomponent materials as evaporated systems for coating deposition slows down diffusion processes, decomposes the solid solution with the formation of chemical compounds, and, consequently, reduces the entropy of mixing.

[†] **Cite as:** V.M. Beresnev, S.V. Lytovchenko, M.O. Azarenkov, O.V. Maksakova, D.V. Horokh, B.O. Mazilin, East Eur. J. Phys. 3, 279 (2023), <https://doi.org/10.26565/2312-4334-2023-3-25>

© V.M. Beresnev, S.V. Lytovchenko, M.O. Azarenkov, O.V. Maksakova, D.V. Horokh, B.O. Mazilin, 2023

Among the proven physical technologies for obtaining such coatings, the ion-plasma technologies (magnetron sputtering as well as vacuum-arc deposition) are the most widely used. The specific characteristics of these technologies significantly affect the structural-phase state of the formed coatings, which, in turn, determines the achieved physical and mechanical characteristics [7–11].

The crucial physical and technological parameters of deposition that affect the microstructure and physical and mechanical properties of coatings are the magnitude of the negative bias potential applied to the substrate, the partial pressure of the reaction gas in the chamber, as well as the amount, concentration, and type of alloying elements. It is known that the addition of silicon to two- or three-element coatings based on titanium nitride, aluminum nitride, and zirconium nitride increases the thermal stability of the nanostructural state by thermodynamically controlled segregation of secondary phases that are insoluble in the volume of crystalline grains [12]. The high hardness of such coatings is due to the fact that at grain sizes between 5 to 8 μm , the generation and propagation of dislocations are not possible, the crack propagation and grain boundary sliding are suppressed, and the yield stress has a value close to the theoretical shear resistance.

It is known, the addition of yttrium to the coating promotes an increase in the resistance to oxidation due to the formation of the YO_x phase at the grain boundaries [13, 14]. In addition, this element leads to grain crushing and destruction of the columnar microstructure of condensates, which is important for improving friction wear resistance when operating in an oxidizing environment. In this regard, the use of yttrium as an alloying element to improve the thermal and mechanical properties of nitride multicomponent systems is of scientific and practical interest.

In order to develop modern ideas about the physical processes of the formation of multicomponent nitride coatings of (TiZrSiY)N-type under highly nonequilibrium conditions of the vacuum-arc deposition, in this paper, we consider the effect of the nitrogen partial pressure on the structural-phase state (surface morphology, elemental and phase composition), as well as the tribo-mechanical characteristics of the formed coatings.

EXPERIMENT DESCRIPTION

The all-metal target material was obtained by vacuum-arc melting in a cooled copper mold. The ingot was produced by pre-mixing the required amount of alloy components, followed by fusion in a high-purity inert gas atmosphere. To achieve the most uniform distribution of the metal components, the vacuum-arc melting of the target material was carried out five times, and after each melting, the ingot was turned over in the mold. Then, the target cathode was made from the obtained ingot. Before coatings deposition for several minutes in an argon atmosphere, a surface layer was preliminarily sputtered from the cathode to remove oxide films formed during the manufacture of the cathode.

Experimental coatings were formed by vacuum arc deposition [15] by evaporation the all-metal target with the following composition of elements (in at %): 72.5 Ti + 20.0 Zr + 5.0 Si + 2.5 Y. The substrates of 18 mm in width, 18 mm in length, and 2.5 mm in thickness were made of steel 12X18H9T (world analogues: USA 321, Japan SUS321, SUS321TK, United Kingdom 321S51). Technological parameters of coating deposition are submitted in Table 1.

Table 1. Physical and technological parameters adjusted during deposition of multicomponent (TiZrSiY)N coatings

Series No	I_d , A	I_f , A	U_b , V	P_N , Pa	h
1	100	0.5	-200	0.08	1
2				0.2	
3				0.55	

Note: I_d – arc current, I_f – focus coil current, U_b – negative bias potential, P_N – nitrogen pressure, h – deposition time.

Microscopic examination of the surface and cross-section of the coatings was carried out using a scanning electron microscope Nova NanoSEM 450. The thickness of the coatings was measured based on the cross-section images.

The elemental composition of the coatings was determined from the spectra of characteristic X-ray radiation generated by an electron beam in a scanning microscope. The spectra were obtained using an EDAX PEGASUS energy-dispersive X-ray spectrometer installed in a Nova NanoSEM 450 microscope.

The surface topography of the coatings was analyzed using an atomic force microscope produced by NT-MDT company.

The phase composition and sub-structural studies were carried out on an X-ray diffractometer DRON-3M in filtered $\text{Cu-K}\alpha$ radiation ($\lambda = 1.54060 \text{ \AA}$, 45 kV and 40 mA) using a graphite monochromator in the secondary beam. Diffraction spectra were taken in the scheme of θ - 2θ scanning with Bregg-Brentano focusing.

The Vickers hardness and the elastic modulus of the coatings were measured on a Shimadzu HMV-G21S instrument. The load was 245.2 mN, the holding time was 10 seconds, the distance between the measurement points was 40 microns. The number of measurements was 10 for each sample, and the average values were calculated in the final.

The adhesive/cohesive strength of the coatings was determined by nanoscale scratching using a Revetest scratch tester (CSM Instruments) in progressive load testing mode. During the tests, changes in the friction coefficient and acoustic emission were recorded, as well as the main critical loads were identified. The following classification of the critical load was chosen: Lc1 is the formation of the first chevron crack at the bottom and diagonal cracks at the edges

of the scratch; Lc2 is the formation of a group of chevron cracks at the bottom of the scratch; Lc3 is the local failure of the coating after the formation of a group of chevron cracks at the bottom of the scratch; Lc4 is the cohesive-adhesive destruction of the coating; Lc5 is the plastic wear of the coating to the base [16]. The critical load Lc5 corresponding to the load when the destruction of the coating occurred, was taken as the criterion for the adhesive strength index.

RESULTS AND DISCUSSIONS

The surface morphology and cross-section of one of the experimental coatings are shown in Figures 1a and 1b. A significant amount of the craters, droplet fraction and solidified macroparticles of the sputtered cathode was fixed on the surface, which is typical for the vacuum-arc deposited materials obtained from unseparated plasma flows [15]. The increase in the size of particles of the droplet fraction, as well as their tendency to agglomerate, is apparently associated with the erosion of zirconium. The data of different authors on the erosion coefficient of Zr are somewhat different while indicating that the erosion index for Zr is significantly exceed the erosion coefficients of Ti, Mo, and W [17]. The droplets exist in two main forms: a flat shape when their surface is parallel to the coating and a spherical shape, which is bulging with respect to the coating. The different shapes of droplets are probably formed from materials of different phases. Spherical droplets show the correct geometric shape. Around them, there are regular circles on the surface of the coating. The flat shape droplets have a microstructure of the surface, similar to the microstructure of the coating. According to the visual analysis of the boundary between the flat droplet and the coating, it seems that there is a strong mechanical connection between them. Similar shapes of the droplets on Zr-Si-N coatings deposited by the arc evaporation at different substrate bias voltages were observed in [18]. During tribological investigations using microtribometers, these droplets directly influence the results as they are deformed, pulled out from the coating surface, and participate in the friction process as so-called a third body.

The cross-sectional image shown in Figure 1b was used to measure the coating thickness. The thickness was found to be 7.37 microns. It is also obvious, that the interface between the steel substrate and the coatings is rather clear, the coating repeats the shape of the substrate very fine. There are no voids or cracks, thus, the adhesion of the coating to the based material (substrate) is supposed to be high. The small inclusions of metal drops are visible within the cross-section image, but they did not cause any structural destruction. In this case, we can summaries that the deposition of the experimental coatings went well and the structural integrity is verified.

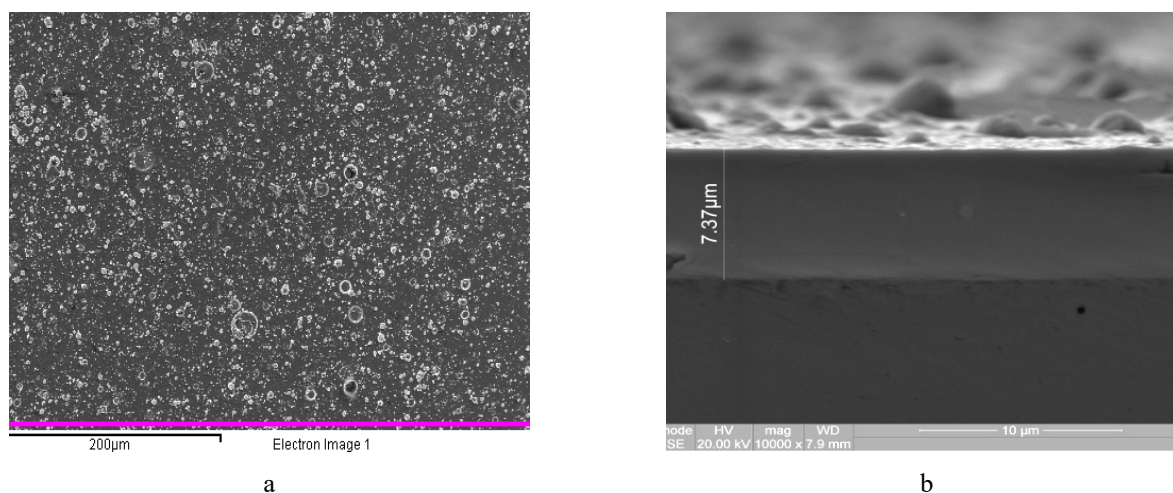


Figure 1. SEM images of the multicomponent (TiZrSiY)N coating obtained at nitrogen pressure 0.55 Pa (series no. 3): surface (a) and cross-section (b)

The chemical composition of the experimental coatings obtained via EDX is summarized in Table 2. From the obtained results, one can see the tendency in the concentration change of the structural elements: Zr, Si, and Y concentrations are lowering with the N pressure increasing. This goes due to the re-sputtering during the deposition process.

Figure 2 shows AFM surface images of the multicomponent (TiZrSiY)N coatings obtained at different nitrogen pressures. These figures confirm the rather complex surface topography of both experimental coatings. A comparison of the surface topography shows that the coating obtained at a lower nitrogen pressure, 0.08 Pa, is characterized by a large amount of a droplet component with a higher peak height and a large height spread.

Table 2. Elemental composition of the multicomponent (TiZrSiY)N coatings by EDX

Series No	Element				
	N	Ti	Zr	Si	Y
Composition, at. %					
1	37.2	46.3	13.4	2.2	0.9
2	43.2	41.9	12.5	1.7	0.7
3	44.2	44.8	9.5	0.9	0.6

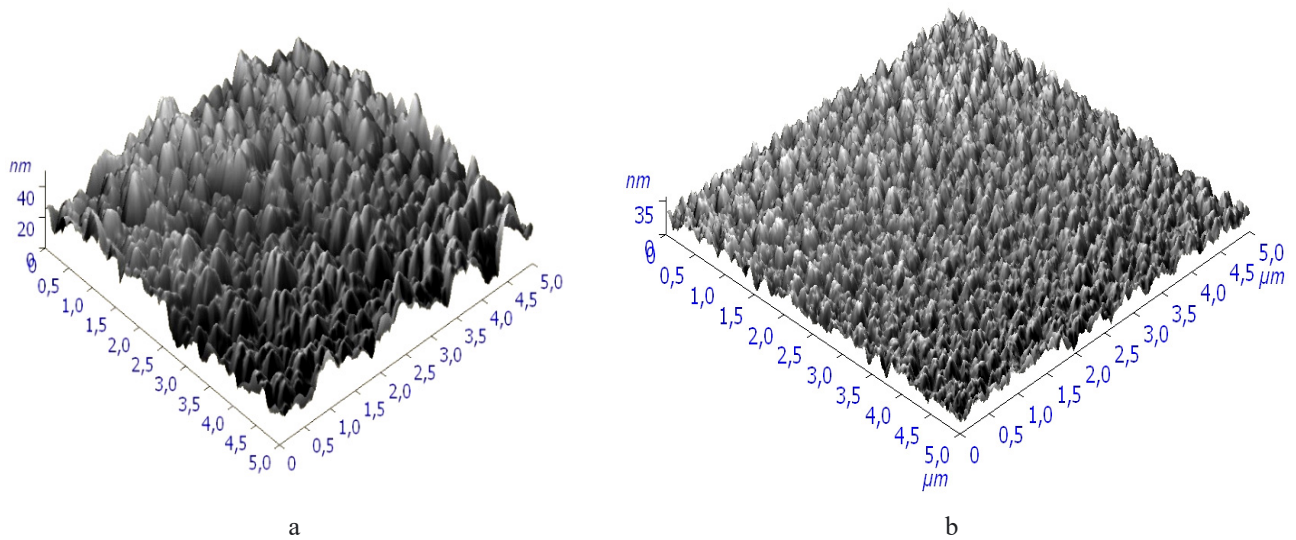


Figure 2. 3D AFM surface images of multicomponent (TiZrSiY)N coatings obtained at nitrogen pressure: 0.08 Pa (series no. 1) (a) and 0,55 Pa (series no. 3) (b)

In the coating obtained at the higher nitrogen pressure of 0.55 Pa, better topography uniformity is observed; the height of the peaks is smaller and the scatter of their heights is also smaller. The change in the surface topography is associated with the processes of the energy impact of particles on the surface. The sufficiently high energy of particles incident on the surface, due to a significant bias potential (-200 V), increases the temperature of the substrate. Due to such heating, diffusion, and recrystallization processes are intensified, which, in turn, leads to the evolution of the phase composition of the near-to-surface layers of the coating and the formation of areas with a reduced stress level [19]. The alternation of dark and light protrusions, cones, and pores of nanosized regions is clearly visible, which indicates a change in the height of individual sections of the surface relief.

At the same time, the high energy of metal particles bombarding the coating at low nitrogen pressure and applying a sufficiently high negative bias potential (-200 V) to the substrate, as well as the large difference in the size of the atoms of the multicomponent system (Table 3), leads to the coating deformation as micro- and at macrolevels and stimulates the formation of rough surface topography for the coating series no. 1.

Table 3. Atomic radius of elements of a multicomponent TiZrSiY coating [19]

Element	Ti	Zr	Si	Y
Radius, nm	0.140	0.155	0.110	0.180

Increasing the nitrogen pressure in the deposition chamber leads to a decrease in the average energy of the evaporated particles (losses during collisions in the interelectrode gap affect) and deformation of the coating, as well as to increase the saturation of the coating with nitrogen atoms. The latter form chemical bonds with the metal base and occupy octahedral interstices characteristic of a NaCl-type crystal lattice, thus preventing shear displacement of the planes with the formation of stacking faults. The mentioned structural changes can lead to an increase in the mechanical properties of the coating, especially hardness, which is expected to see for the samples obtained at the maximum nitrogen pressure of 0.55 Pa.

Figure 3 shows the diffraction patterns of multicomponent (TiZrSiY)N coatings deposited at different partial pressures. A cubic TiN phase (ICCD: 04-001-2272) with a crystal lattice of NaCl-B1 type is formed in all experimental coatings. For all diffraction spectra, the (111) diffraction line has the highest intensity. There are also a number of low-intensity diffraction reflections corresponding to a mixture of (200) + (220) + (311) + (222) oriented grains.

In the coating deposited at nitrogen pressures of 0.08 Pa (see Figure 3a), the presence of cubic TiN and the α -Ti phase was identified. The lattice parameter of TiN nitride is $a = 0.4262$ nm. Calculation of substructural characteristics showed that the crystallite size of titanium nitride is 19.5 nm at the level of microdeformations $\epsilon = 4.66 \cdot 10^{-3}$. The α -Ti lattice in the coating has the following lattice parameters: $a = 0.2968$ nm, and $c = 0.4757$ nm, which exceeds the values known from the scientific sources ($a = 0.29505$ nm, and $c = 0.4697$ nm) [20]. Therefore, the α -Ti phase is probably a solid solution of nitrogen in titanium.

The coating obtained at nitrogen pressure of 0.2 Pa (see Figure 3b) contain the same phases: cubic titanium nitride TiN and α -Ti. The lattice parameter of TiN nitride is $a = 0.4268$ nm, while the crystallite size is larger and equal to 26.5 nm at the lower level of microstrains $\epsilon = 4.27 \cdot 10^{-3}$. The lattice parameters of the α -Ti phase is the same as for the coatings obtained at nitrogen pressure of 0.08 Pa.

In the coatings obtained at nitrogen pressure of 0.55 Pa (see Figure 3c), one phase was identified as cubic titanium nitride, TiN, with a lattice parameter $a = 0.4291$ nm and the largest crystallite size of 34.9 nm at the lowest microdeformation level $\epsilon = 3.79 \cdot 10^{-3}$.

It is known that the value of the texture coefficient $T_{C(hkl)}$ is proportional to the number of crystallites (grains) that are oriented in a certain crystallographic direction. In cases of $T_{C(hkl)} > 1$, a large number of crystallites are oriented to a certain crystal plane. When $T_{C(hkl)} \leq 1$, the opposite variant is observed – a significant disorientation of crystallites. The calculated texture coefficient of the coating obtained at nitrogen pressure of 0.55 Pa is 5.95. This coating is characterized by the highest level of texturing compared to the coatings obtained at a lower nitrogen pressure ($T_{C(hkl)} = 3.50$ for the coating obtained at nitrogen pressure of 0.08 Pa, and $T_{C(hkl)} = 4.99$ for the coating obtained at nitrogen pressure of 0.2 Pa).

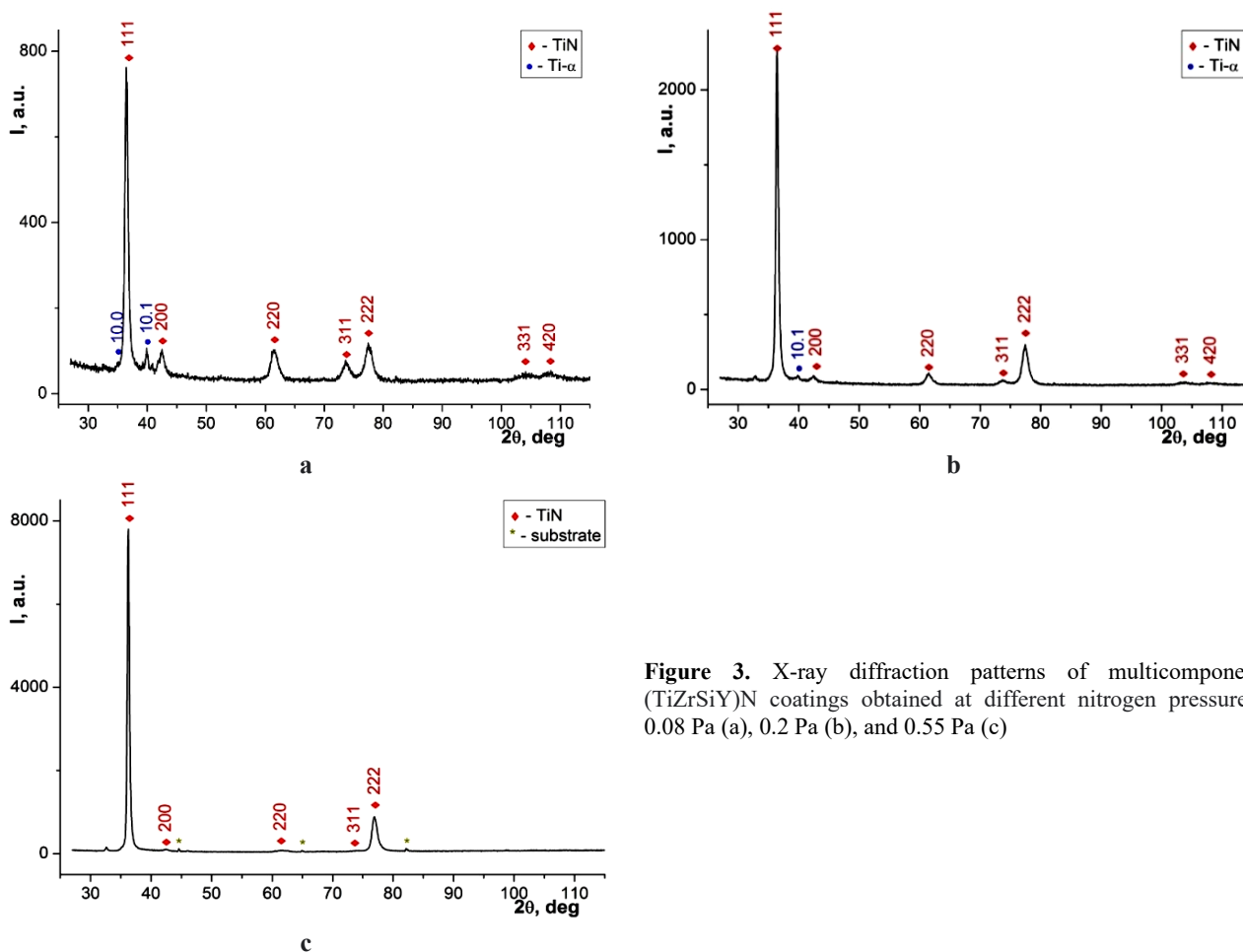


Figure 3. X-ray diffraction patterns of multicomponent (TiZrSiY)N coatings obtained at different nitrogen pressures: 0.08 Pa (a), 0.2 Pa (b), and 0.55 Pa (c)

One of the most important mechanical characteristics of multicomponent coatings are hardness (H) and elastic modulus (E). The results of measuring the abovementioned parameters as well as calculated values of the elastic strain to failure (H/E) and the resistance to plastic deformation (H^3/E^2) are shown in Table 4.

Table 4. Mechanical characteristics of multicomponent (TiZrSiY)N coatings

Series No.	Vickers hardness H, GPa	Elastic modulus E, GPa	H/E	H^3/E^2
1	25	284	0.088	0.19
2	31	327	0.09	0.27
3	36	347	0.1	0.38

The improvement in all mechanical properties with an increase in nitrogen pressure is obvious. Moreover, the coating series no. 3 has the smoothest surface. This means that the coating structure is denser, and, therefore, the hardness is higher.

Generally, such high mechanical properties of the experimental coatings are probably due to the complex influence of several effects, in particular, (1) the nanosize of grains, (2) the formation of a close-packed crystallite texture with the [111] axis, (3) the surface roughness, and (4) a certain level of internal stresses.

For the operational characteristics of coatings, an important criterion is their adhesive strength. In this work, the scratch testing method was used to determine the adhesive strength parameters of the coatings (see Figures 4 and 5). Based on the tests results, the coefficient of friction at different stages of wear, the amplitude of acoustic emission, as well as the critical loads were determined.

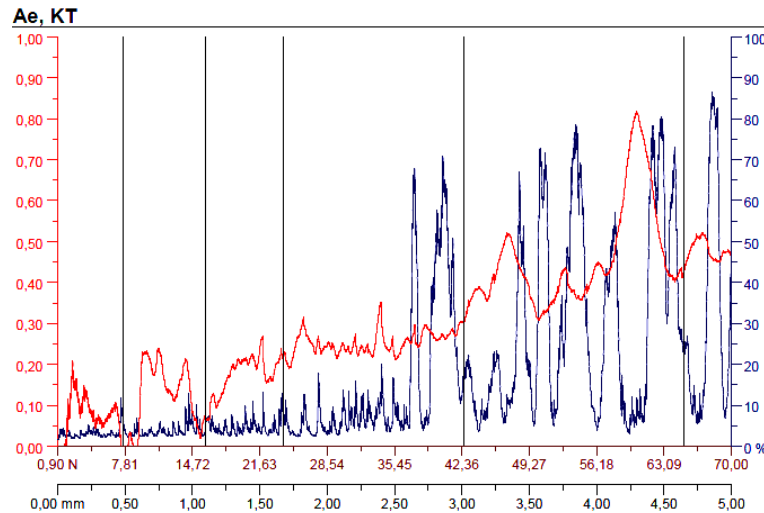


Figure 4. The graph of wear parameters obtained for the multicomponent (TiZrSiY)N coating obtained at nitrogen pressure 0.55 Pa (series no. 3): the coefficient of friction KT (red line, left scale), the amplitude of acoustic emission AE (blue line, right scale), the normal load to the indenter (brown bottom scale), the length of the scratch (black bottom scale)

A significant scatter in the values of the friction coefficient is due to the presence of a droplet fraction on the surface of the particles, which have micron sizes and create a large roughness. The composition of these particles differs greatly from the composition of the main coating layer; therefore, the interaction with the moving indenter also changes, which confirms the change of the course of the friction coefficient curve.

An analysis of the change in the level of the acoustic emission signal shows that the process of accumulation of cracks when approaching the load Lc4 leads to a sharp increase in acoustic emission (approximately 5-7 times), the level of which continues to slightly increase with further loading.

Microscopic images of the scratch at different critical loads for multicomponent (TiZrSiY)N coating obtained at nitrogen pressure of 0.55 Pa is presented in Figure 5.

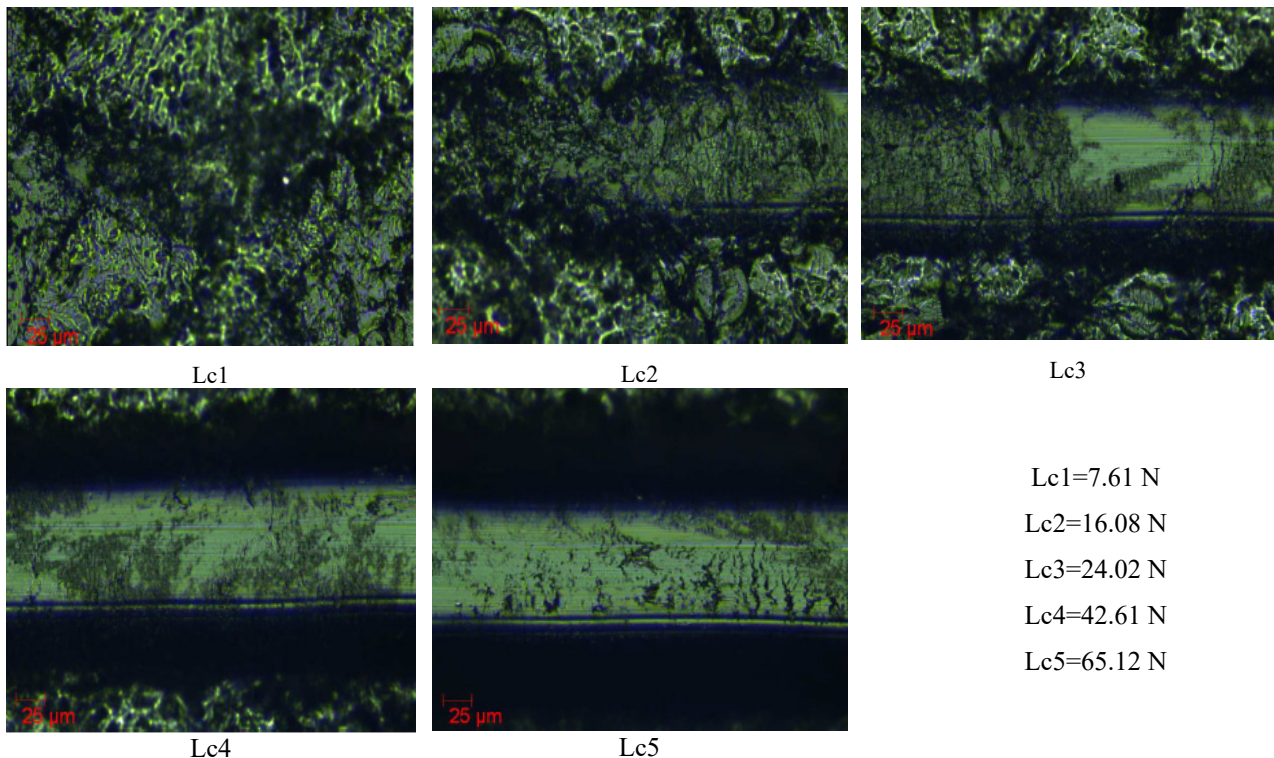


Figure 5. Microscopic images of the scratch at different critical loads for multicomponent (TiZrSiY)N coating obtained at nitrogen pressure of 0.55 Pa (series no. 3)

Table 5 shows the results of adhesion tests of all multicomponent coatings. It is obvious that the coating obtained at the highest nitrogen pressure of 0.55 Pa is characterized by higher critical loads (Lc1-Lc5) compared to other coatings.

Table 5. Critical load values (N) for multicomponent (TiZrSiY)N coatings

Series No.	Lc1	Lc2	Lc3	Lc4	Lc5
1	4.1	12.8	19.9	29.8	42.3
2	6.9	14.8	21.1	38.4	56.2
3	7.6	16.1	24.2	42.6	65.1

When scratching, the coatings are abraded, but do not exfoliate, i.e., they are destroyed by the cohesive mechanism associated with plastic deformation and the formation of fatigue cracks in the coating material. The difference in the level of adhesive strength of the coatings is due, on the one hand, to mechanical interaction due to the roughness of the contacting surfaces, and on the other hand, to chemical-interatomic interaction at the interface of the contacting bodies. In this case, the process of accumulation of cracks and local flaking (at Lc4) occurs in the coating in a rather narrow area of loads, and a large area corresponds to the abrasion of the coating to the substrate (at Lc4 - Lc5).

CONCLUSIONS

Multicomponent (TiZrSiY)N coatings formed using vacuum-arc technique at different nitrogen pressures were investigated. The analysis of the results of the phase composition and surface morphology suggests as follows:

1. During the formation of coatings under conditions of low nitrogen pressure, cubic titanium nitride TiN with the {111} texture and titanium (in the form of a solid solution) were identified.
2. Increasing the nitrogen pressure leads to an increase in the lattice parameter of TiN. In this case, an increase in the crystallite size of titanium nitride and a decrease in the level of microdeformations are observed. The {111} texture in titanium nitride also becomes stronger with increasing nitrogen pressure.
3. With the increase in the partial pressure of nitrogen in the coating, the texture coefficient increases to 5.795, which is associated with the formation of a more perfect substructure and the formation of a larger amount of crystallites with minimal defects.
4. The microhardness of multicomponent (TiZrSiY)N coatings increases with increasing nitrogen pressure during deposition from 25.0 GPa (at the nitrogen pressure of 0.08 Pa) to 36.0 GPa (at the nitrogen pressure of 0.55 Pa).
5. Studies of the process of destruction of coatings indicate that, depending on the structural-phase state of the coatings, their adhesive strength changes. Adhesive destruction of a multicomponent coating obtained at the highest nitrogen pressure of 0.55 Pa occurs at a load of 65.12 N.
6. According to the complex of parameters, H, E, H/E, H³/E², friction coefficient and critical loads, the presented multicomponent (TiZrSiY)N coatings can be very attractive for tribological application.

Acknowledgements

This work was supported by the National Research Foundation of Ukraine in the framework of the project No 2020.02/0234.

ORCID

- Vyacheslav M. Beresnev, <https://orcid.org/0000-0002-4623-3243>;
 ● Serhiy V. Lytovchenko, <https://orcid.org/0000-0002-3292-5468>
 ● Mykola O. Azarenkov, <https://orcid.org/0000-0002-4019-4933>;
 ● Olga V. Maksakova, <https://orcid.org/0000-0002-0646-6704>
 ● Denis V. Horokh, <https://orcid.org/0000-0002-6222-4574>;
 ● Bohdan O. Mazilin, <https://orcid.org/0000-0003-1576-0590>

REFERENCES

- [1] A.D. Pogrebnjak, A.A. Bagdasaryan, I.V. Yakushchenko, and V.M. Beresnev. Russ. Chem. Rev. **83**, 1027 (2014), <https://dx.doi.org/10.1070/RCR4407>.
- [2] W. Li, P. Liu, and P.K. Liaw. Mater. Res. Lett. **6**(4), 199 (2018). <https://doi.org/10.1080/21663831.2018.1434248>.
- [3] J. Li, Y. Huang, X. Meng, and Y. Xie. Adv. Eng. Mater. **21**, 1900343 (2019). <https://doi.org/10.1002/adem.201900343>.
- [4] E. Lewin. J. Appl. Phys. **127**(16) 160901 (2020) <https://doi.org/10.1063/1.5144154>.
- [5] U.S. Nyemchenko, V.M. Beresnev, O.V. Sobol, S.V. Lytovchenko, V.A. Stolbovoy, V.J. Novikov, A.A. Meylekhov, A.A. Postelnyk, and M.G. Kovaleva. PAST, **101**, 112 (2016). https://vant.kipt.kharkov.ua/ARTICLE/VANT_2016_1/article_2016_1_112.pdf
- [6] T. Ikeda, and H. Satoh, Thin Solid Films, **195**(1-2), 99 (1999). [https://doi.org/10.1016/0040-6090\(91\)90262-V](https://doi.org/10.1016/0040-6090(91)90262-V)
- [7] A.D. Pogrebnjak, A.P. Shpak, N.A. Azarenkov, and V.M. Beresnev, Physics-Uspekhi, **52**(1), 29 (2009). <https://doi.org/10.3367/UFNe.0179.200901b.0035>
- [8] A.D. Pogrebnjak, and V.M. Beresnev, in: *Nanocomposites – New Trends and Developments*, edited by Farzad Ebrahimi (InTech, 2012), pp. 123-160, <https://doi.org/10.5772/3389>
- [9] O.V. Maksakova, V.M. Beresnev, S.V. Lytovchenko, and D.V. Horokh, in: *2022 12th International Conference Nanomaterials: Applications & Properties* (IEEE, Krakow, Poland, 2022), pp. 01-06, <https://doi.org/10.1109/NAP55339.2022.9934659>
- [10] S. Veprek, M. Veprek-Heijman, P. Karvankova, and J. Prochazka. Thin Solid Films, **476**, 1-29 (2005). <https://doi.org/10.1016/j.tsf.2004.10.053>
- [11] J. Musil, P. Banoch, and P. Zeman, in: *Plasma Surface Engineering and Its Practical Applications*, edited by R. Wei (Research Signpost Publisher, USA, 2007), pp. 1-35.
- [12] P.J. Martin, A. Bendavid, J.M. Cairney, and M. Hoffman. Surf. and Coat. Technol. **200**(7), 2228 (2005). <https://doi.org/10.1016/j.surfcoat.2004.06.012>

- [13] V.M. Beresnev, O.V. Sobol', A.D. Pogrebnyak, S.V. Lytovchenko, O.N. Ivanov, U.S. Nyemchenko, P.A. Srebniuk, A.A. Meylekhov, A.Ye. Barmin, V.A. Stolbovoy, V.Yu. Novikov, B.A. Mazilin, E.V. Kritsyna, T.A. Serenko, and L.V. Malikov, PAST, **110**, 88 (2017). https://vant.kipt.kharkov.ua/ARTICLE/VANT_2017_4/article_2017_4_88.pdf
- [14] V. Belous, V. Vasyliiev, A. Luchaninov, V. Marinin, E. Reshetnyak, V. Strel'nitskij, and S. Goltvyanytsya, Surf. and Coat. Techn. **223**, 68 (2013). <https://doi.org/10.1016/j.surfcoat.2013.02.031>
- [15] I.I. Aksenov, and D.S. Aksyonov, East Eur. J. Phys. **1**(3), 22 (2014). <https://doi.org/10.26565/2312-4334-2014-3-02>
- [16] J. Valli, Journ. of Vac. Sci. and Technol. **A4**, 3007 (1986). <https://doi.org/10.1116/1.573616>.
- [17] J. E. Daalder. Journ. of Phys. D: Appl. Phys. **8**, 1647 (1975). <https://dx.doi.org/10.1088/0022-3727/8/14/009/>
- [18] B. Warcholinski, T.A. Kuznetsova, A. Gilewicz, T.I. Zubar, V.A. Lapitskaya, S.A. Chizhik, A.I. Komarov, et al., J. of Materi. Eng. and Perform. **27**, 3940-3950 (2018). <https://doi.org/10.1007/s11665-018-3483-7>
- [19] J.C. Slater, Journ. of Chem. Phys. **41**(10), 3199 (1964). <https://doi.org/10.1063/1.1725697>
- [20] D.R. Lide, editor, *CRC Handbook of Chemistry and Physics*, 90th edition (CRC Press/Taylor & Francis, 2009).

**БАГАТОКОМПОНЕНТНІ ПОКРИТТЯ НА ОСНОВІ СИСТЕМИ (TiZrSiY)N,
ОТРИМАНІ МЕТОДОМ ВАКУУМНО-ДУГОВОГО ОСАДЖЕННЯ
В'ячеслав М. Береснев^а, Сергій В. Литовченко^а, Микола О. Азаренков^{а,б},
Ольга В. Максакова^а, Денис В. Горох^а, Богдан О. Мазілін^а**

^аХарківський національний університет імені В.Н. Каразіна, майдан Свободи 4, 61022, м. Харків, Україна

^бНаціональний науковий центр «Харківський фізико-технічний інститут», вул. Академічна, 1, 61108, м. Харків, Україна

Вивчено вплив тиску реакційного газу (азоту) на структурно-фазовий стан та властивості вакуумно-дугових нітридних покриттів системи (TiZrSiY)N. На поверхні покриттів спостерігається значна кількість краплинної фракції та затверділих макрочастинок розпорошеного катода, що є характерним для вакуумно-дугових конденсатів, які осаджують з несепарованих плазмових потоків. В усіх зразках у покритті зафіксовано нітрид титану з кубічними ГЦК-гратами. У зразках покриттів, осаджених при тисках азоту P_N 0,08 Па і 0,2 Па, також ідентифікована фаза α -Ti, при цьому вимірюваний параметр ґратів цієї фази дозволяє припустити, що ця фаза є твердим розчином азоту в титані. Коефіцієнт текстурі багатоконпонентного покриття, сформованого при потенціалі зміщення -200 В і $P_N = 0,55$ Па має високе значення $T_{C(hkl)} = 5,95$ в порівнянні з іншими зразками. Мікротвердість багатоконпонентних покриттів зростає залежно від парціального тиску азоту від 25,0 до 36 ГПа. Найвищу адгезійну міцність також має покриття, сформоване при найбільшому використаному тиску азоту $P_N = 0,55$ Па.

Ключові слова: вакуумно-дугові покриття; багатоконпонентні нітридні покриття; парціальний тиск азоту; текстура; мікротвердість; адгезійна міцність